








## RESEARCH ARTICLE

# Upgrading of the general AMBER force field 2 for fluorinated alcohol biosolvents: A validation for water solutions and melittin solvation

Michele Casoria<sup>1,2</sup>  | Marina Macchiagodena<sup>1</sup>  | Paolo Rovero<sup>2,3</sup>  |  
Claudia Andreini<sup>1,4</sup>  | Anna Maria Papini<sup>1,2</sup>  | Gianni Cardini<sup>1</sup>  | Marco Pagliai<sup>1</sup> 

<sup>1</sup>Dipartimento di Chimica "Ugo Schiff",  
Università degli Studi di Firenze, Sesto  
Fiorentino, Italy

<sup>2</sup>Interdepartmental Research Unit of Peptide  
and Protein Chemistry and Biology, Università  
degli Studi di Firenze, Sesto Fiorentino, Italy

<sup>3</sup>Department of NeuroFarBa, Università degli  
Studi di Firenze, Sesto Fiorentino, Italy

<sup>4</sup>Magnetic Resonance Center (CERM),  
Università degli Studi di Firenze, Sesto  
Fiorentino, Italy

**Correspondence**

Marina Macchiagodena, Dipartimento di  
Chimica "Ugo Schiff", Università degli Studi di  
Firenze, Via della Lastruccia 3-13, I-50019  
Sesto Fiorentino, Italy.  
Email: [marina.macchiagodena@unifi.it](mailto:marina.macchiagodena@unifi.it)

**Funding information**

European Union - NextGenerationEU,  
Grant/Award Number: CUP  
B83C22002830001

The standard GAFF2 force field parameterization has been refined for the fluorinated alcohols 2,2,2-trifluoroethanol (TFE), 1,1,1,3,3,3-hexafluoro-2-propanol (HFIP), and 1,1,1,3,3,3-hexafluoropropan-2-one (HFA), which are commonly used to study proteins and peptides in biomimetic media. The structural and dynamic properties of both proteins and peptides are significantly influenced by the biomimetic environment created by the presence of these cosolvents in aqueous solutions. Quantum mechanical calculations on stable conformers were used to parameterize the atomic charges. Different systems, such as pure liquids, aqueous solutions, and systems formed by melittin protein and cosolvent/water solutions, have been used to validate the new models. The calculated macroscopic and structural properties are in agreement with experimental findings, supporting the validity of the newly proposed models.

**KEYWORDS**

biomimetic solvents, force field, GAFF2, HFA, HFIP, melittin, molecular dynamics simulation, TFE

## 1 | INTRODUCTION

The presence of fluorinated alcohols as cosolvents has a significant impact on the structural and dynamic properties of proteins and peptides in aqueous solutions.<sup>1</sup> The alcohols most commonly used as cosolvents to create a biomimetic medium are 2,2,2-trifluoroethanol (TFE), 1,1,1,3,3,3-hexafluoro-2-propanol (HFIP), and 1,1,1,3,3,3-hexafluoropropan-2-one (HFA) (structures in Figure 1). The efficacy of structure-inducing cosolvents depends on their concentration in aqueous solution, on particular amino acid sequences, and on the structures involved in the stabilization of the protein or peptide under investigation. Although helical structures have been stabilized more frequently than other motifs such as  $\beta$ -turns,

$\beta$ -hairpins, and  $\beta$ -sheets, these motifs have also been observed to be stabilized.<sup>2</sup> The mixed water-alcohol solvents may approximate the dielectric constant of protein interiors.<sup>1</sup> In the case of peptides derived from protein fragments, the folding in these solutions shows an intrinsic tendency to adopt the secondary structure of the corresponding protein region, which is otherwise unstructured in an aqueous solution.<sup>3</sup> With the exception of HFA, the static dielectric constant,  $\epsilon_r$ , has been determined experimentally.<sup>4</sup> In aqueous solutions, the  $\epsilon_r$  decreases linearly with increasing alcohol concentration. The hydrophobic interactions that stabilize the compact native structure of proteins are weakened by this lower polarity, but interactions such as hydrogen bonding are strengthened, stabilizing secondary structures, especially the *alpha*-helix.

This is an open access article under the terms of the [Creative Commons Attribution-NonCommercial-NoDerivs](https://creativecommons.org/licenses/by-nc-nd/4.0/) License, which permits use and distribution in any medium, provided the original work is properly cited, the use is non-commercial and no modifications or adaptations are made.

© 2023 The Authors. *Journal of Peptide Science* published by European Peptide Society and John Wiley & Sons Ltd.

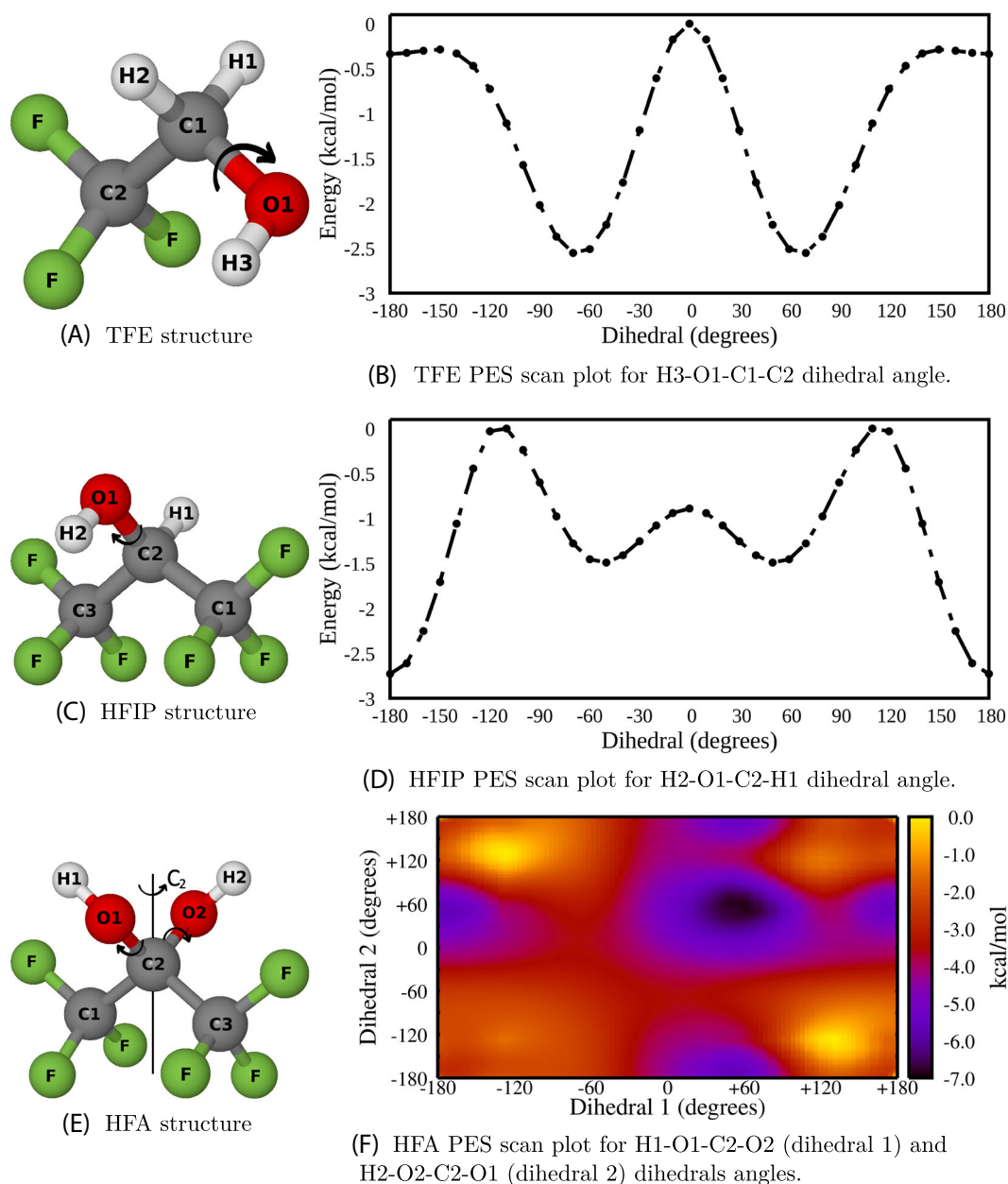


**FIGURE 1** (A, C, and E) Representation of lowest energy conformer, the indication of the dihedral angle used for the PES scan and atom labeling for TFE, HFIP, and HFA, respectively; (B, D, and F) PES scan for selected dihedral angles. The energy values (kcal/mol) are reported as differences against the maximum value. The HFIP conformer shown in (C) corresponds to the antiperiplanar conformation; the HFA conformer shown in (E) corresponds to the symmetrical C2.

Since its discovery by Goodman and coworkers,<sup>5</sup> TFE has been widely used as a cosolvent; its helix-enhancing effect has found many applications, most recently in the NMR-based characterization of short sequences derived from natural proteins. As a general trend, HFIP and HFA are considered stronger structural inducers than TFE, suggesting that cosolvent ability is correlated with the presence of fluorine atoms.<sup>6,7</sup> Using IR-spectroscopy, it has been observed<sup>8</sup> that TFE can reduce the number of hydrogen bonds that the peptide backbone forms with water; desolving the backbone groups in the helical conformation also strengthens intrahelical hydrogen bonds, which

stabilizes the helix. TFE also reduces solvent-backbone hydrogen bonding to helical residues but not to random coil residues. Efforts were made to understand the mechanisms involving these cosolvents in stabilizing the secondary structure.<sup>9,10</sup> Molecular dynamics (MD) simulations are particularly effective in studying the structural and dynamic properties of proteins and peptides in biomimetic media at the molecular level. To accurately reproduce experimental findings, MD simulations need an accurate force field (FF), which is characterized by a set of functional forms with a minimal set of adjustable parameters. Except for HFA, several FFs have been proposed for

cosolvent molecules. TFE in particular has been studied extensively. A first model was reported by van Buuren and Berendsen<sup>11</sup> for GROMOS87 FF,<sup>12</sup> to which fluorine atom parameters were added based on experimental values published in the literature.<sup>13</sup> Another model, proposed by Bodkin and Goodfellow,<sup>14</sup> used bond stretching and Lennard-Jones parameters previously reported in the literature and revised atomic charges. Starting from a model similar to GROMOS96 FF,<sup>15</sup> Fioroni et al.<sup>16</sup> used the same bond length and angle values as in the van Buuren and Berendsen model.<sup>11</sup> The methylene groups were considered as a single united atom; polarization was implicitly included in the assigned partial charges; geometry optimizations at the self-consistent field (SCF) level were carried out using Hartree-Fock (HF) level of theory and with a 6-31G(p,d) basis set. Partial atomic charges were calculated at the RHF and MP2 levels using the CHELPG procedure to perform the electrostatic potential fits. A first comparison of the previously described FFs<sup>17</sup> suggests that all the models have a mixing enthalpy larger than the experimental data, due to weak TFE/water interactions. Furthermore, this comparison shows that Fioroni's model is the best. Other models have been proposed gradually; Scharge et al.<sup>18</sup> with the aim to study small clusters of TFE developed a TFE model for AMBER FF.<sup>19,20</sup> Jia et al.<sup>21</sup> reported a model for TFE using general AMBER force field (GAFF).<sup>22</sup> In 2014, Vymetal and Vondrášek<sup>23</sup> reported a refinement of the GAFF TFE model suitable for simulations in solution with the TIP4P/Ew and TIP4P/2005 water models.<sup>24</sup> The calculated properties, such as density, heat of vaporization, dipole moment, and coefficient of thermal expansion, are in good agreement with the experimental measurements, according to an analysis of the simulation results using GAFF<sup>23</sup>; others, however, differ significantly from the experimental values, including the diffusion constant, heat capacity, static relative permittivity, and isothermal compressibility. Considering HFIP, a first model was proposed by Kinugawa and Nakanishi<sup>25</sup> using HF approximation and STO-3G basis set for geometry optimization. Fioroni et al.<sup>26</sup> reported a model based on GROMOS96 FF. This model considered two conformers: the synclinal (syn) (H2-O1-C2-H1 dihedral angle equal to 60°; for atom labeling, see Figure 1) and the antiperiplanar (ap) (H2-O1-C2-H1 dihedral angle equal to 180°; for atom labeling, see Figure 1). The first is characterized by a weak intramolecular hydrogen bond between a fluorine atom and the hydroxyl hydrogen atom, and the ap conformer is chosen for its lower energy to generate atomic charges.

A specific FF for HFA is not mentioned in the literature. Experimentally, it is known to form stable hydrates. The monohydrate is a solid that melts at 46° C; instead, the trihydrate can be distilled and melts at -11° C. These hydrates are formed by leading gaseous HFA into water. If the molar ratio of the components in the solution is 1:1, only the monohydrate is formed. Hydrated fluoro ketones can be considered fluoro alcohols since they are geminal diols. The additional oxygen atom increases the acidity (pKa = 6.58).<sup>27</sup> The molecular structure of HFA in the gas phase was studied by Tayyari et al.<sup>28</sup> at B3LYP/6-311G\* level of theory, suggesting the symmetrical C<sub>2</sub> as major conformer (structure in Figure 1E).

In the absence of a specific FF for HFA, we present here a parameterization of the FF for HFA and a reparameterization for TFE and HFIP biosolvents using GAFF2<sup>22</sup> parameters. GAFF2 is the second generation on GAFF and an ongoing project aimed at obtained high-quality parameters to reproduce experimental finding. New atomic charges are also generated using ab initio calculations. Moreover, with respect to the just described FFs, the chosen method allows to obtain parameters that can be used in conjunction with the AMBER FF<sup>29</sup> parameterization for peptides. The obtained parameters are examined by running MD simulations of two water-cosolvent solutions: one with one cosolvent molecule and 500 water molecules and another with a 50:50 (v/v) water-cosolvent solution. We also perform MD simulations of melittin (MLT), a component of the venom of *Apis mellifica*, in water and in 50:50 (v/v) water-cosolvent solutions. MLT is a 26-mer peptide that is unfolded in water at low pH<sup>30</sup> but assumes an  $\alpha$ -helical conformation when it is bound to the membrane as well as in alcohols solutions.<sup>31</sup> In particular, MLT consists of two  $\alpha$ -helical regions, and these portions are connected by the residues Thr-11 and Gly-12. The value of the bend angle between the two  $\alpha$ -helix ranges from 120° to 160°. To confirm the effect of the atomic charge parameterization, the results for MLT were also compared.

## 2 | METHODS

### 2.1 | Force field parametrization

GAFF2, obtained using the PrimaDORAC web interface,<sup>32,33</sup> was used for bonded (stretching, bending, and dihedral angle FF terms) and Lennard-Jones parameters. For atomic charges, we compare three different sets: standard GAFF2, Mulliken, and RESP.<sup>34</sup> The standard GAFF2 atomic charges are directly derived using the PrimaDORAC web interface<sup>33</sup>; the Mulliken ones are parametrized<sup>35</sup> using density functional theory (DFT) calculations, performed at B3LYP/6-31+G(d) level of theory using Gaussian09 software<sup>36</sup> and the conductor-like polarizable continuum model (C-PCM) to describe the bulk solvent effects<sup>37</sup>; the RESP atomic charges are derived using HF-SCF method and the 6-31G\* basis set.<sup>38</sup> The atomic charges are calculated on the lowest energy conformer that was been identified using single-point energy evaluations on a selected dihedral angle at predetermined steps for each of the cosolvent molecules, HFA, HFIP, and TFE. The potential energy surface (PES) scan of selected dihedral angles has been performed using Gaussian09 software<sup>36</sup> and considering 37 points from -180° to +180°, 1 point each 10°.

\*GAFF and GAFF2 are public domain force fields and are part of the AmberTools23 distribution, available for download at <https://ambermd.org/> (accessed May 2023). According to the AMBER development team, the improved version of GAFF, GAFF2, is an ongoing project aimed at "reproducing both the high-quality interaction energies and key liquid properties such as density, the heat of vaporization and hydration free energy." GAFF2 is expected "to be an even more successful general purpose force field and that GAFF2-based scoring functions will significantly improve the success rate of virtual screenings."

## 2.2 | Molecular dynamics simulations

MD simulations were performed on previously described systems using GROMACS 2021.2.<sup>39</sup> Specifically, 500 molecules were used in the case of a pure cosolvent solution, and 500 TIP3P<sup>40,41</sup> water molecules were used to study a single cosolvent molecule in water mixtures. The total number of molecules in water mixtures containing 50:50 (v/v) ratios of HFA, HFIP, and TFE was 6000 with 780, 840, and 1200 molecules of HFA, HFIP, and TFE, respectively, and the remaining water molecules. The starting coordinates were generated using GROMACS standard tools and inserting a specified number of molecules in random positions. For water/MLT and for each water-cosolvent mixture 50:50 (v/v)/MLT simulation, MLT (pdb identification code 2MLT) was parametrized using AMBER99SB-ILDN FF.<sup>29</sup> In addition, for the first system, water/MLT, 5943 of TIP3P water molecules were used; in the case of MLT in 50:50 (v/v) water-cosolvent solution, we maintain the same proportion of water to cosolvent molecules as in earlier systems. For all systems, simulations were performed using a cubic box (dimensions in Table S1) with periodic boundary conditions.

First, the steepest descent energy minimization was applied. Then, the systems were heated up to 298.15 K for 100 ps while keeping the temperature constant using a Nosé-Hoover approach,<sup>42</sup> with a coupling time constant of 1 ps. The resulting configuration was used as a starting point for NPT simulation (using the Parrinello-Rahman barostat<sup>43</sup> with a period of pressure fluctuations at the equilibrium setting at 2.0 ps) until the systems were allowed to converge to uniform density (100 ps, time-step 2 fs). In addition, for pure and 50:50 (v/v) water-cosolvent mixture systems, we performed MD simulations in the NVT ensemble for 20 ns using the box obtained from the NPT simulation with a time-step equal to 2.0 fs. For the water-cosolvent mixture 50:50 (v/v)/MLT system after the first NPT simulation, we performed a production run of 100 ns with a time-step of 2 fs. For all simulations, electrostatic interactions were evaluated using the particle-mesh Ewald (PME)<sup>44</sup> method with a grid spacing of 1.2 Å, a real-space cutoff of 1.2 nm, and a spline interpolation of order 4. van der Waals interactions were calculated using a cut-off of 1.2 nm. Long-range dispersion corrections for Lennard-Jones interactions were used for energy and pressure.<sup>39,45</sup> In the production run, the LINCS algorithm<sup>46</sup> was used to impose rigid constraints on the X-H bonds (where X is any heavy atom). To calculate the  $\Delta G$  of hydration ( $\Delta G_{hydr}$ ), the standard free energy perturbation (FEP) method was used. The FEP protocol computes the free energy difference between the solvated molecule and the molecule in the gas phase by constructing a pathway during which the interactions (electrostatic and van der Waals) of the molecule with the solvent are decoupled step by step. A soft-core potential, with the formulation introduced by Beutler et al.,<sup>47</sup> is employed to reduce the instability (sc-alpha=0.5, sc-power=1, and sc-sigma=0.25). The Hamiltonian differences were saved in GROMACS dhdl.xvg files and used to obtain the free energy contribution by Bennett's acceptance ratio (BAR) method.<sup>48</sup> In particular, we used seven windows of 2 ns with coupling parameter ( $\lambda$ ) equal to 0.0, 0.2,

0.4, 0.6, 0.8, 0.9, and 1.0, and in the calculation of  $\Delta G_{hydr}$ , we exclude the first 200 ps of the simulations.

## 2.3 | Analysis

Static dielectric constant ( $\epsilon$ ), density ( $\rho$ ), root mean square deviation (RMSD) and root mean square fluctuation (RMSF) were determined using GROMACS standard tools; intermolecular radial distribution functions (RDFs), denoted by  $g_{xy}(r)$ , were obtained using TRAVIS software.<sup>49,50</sup> In particular for  $\epsilon$  calculation, the total dipole plus fluctuations was used for the estimation according to Equation (1):

$$\epsilon = 1 + \frac{4\pi}{3 \langle V \rangle k_B T} (\langle M^2 \rangle - \langle M \rangle^2); M = \sum_i \mu_i \quad (1)$$

where  $\mu_i$  is the molecular dipole moment.

The secondary structure of MLT and its evolution were analyzed using the define secondary structure of proteins (DSSP) algorithm.<sup>51</sup> In order to describe the interaction of the peptide with the cosolvent, the local cosolvent concentration (LCC) was evaluated from the number of solvent and cosolvent molecules present in a shell of 6 Å around the peptide residues.<sup>10</sup> Furthermore, the LCC was evaluated considering shells of different sizes, from 4 Å to 25 Å.

## 3 | RESULTS AND DISCUSSION

### 3.1 | Conformation analysis and atomic charges derivation

The GAFF2, Mulliken, and RESP atomic charges were calculated on the lowest energy conformer derived from the PES scan. The result for each cosolvent is reported in Figure 1. For TFE and HFIP, the scan included only one dihedral angle, H3-O-C1-C2 and H2-O-C2-H1 for TFE and HFIP, respectively. For HFA, we used a two-dimensional PES scan in which the dihedral angles H1-O1-C2-O2 and H2-O2-C2-O1 were scanned. The lowest energy conformer found for HFIP corresponds to the antiperiplanar one (structure in Figure 1C) reported in the paper of Fioroni et al.<sup>26</sup> as the more stable. Also for HFA, we found that the conformer more stable corresponds to one already reported, the symmetrical  $C_2$  (structure in Figure 1E).<sup>28</sup> On the lowest energy conformers structures, we calculated the new atomic charges reported in Table 1, and the corresponding topology file for each cosolvent molecule is provided in Supporting Information.

GAFF2 and RESP atomic charges are comparable; instead, Mulliken atomic charges are significantly higher (in absolute value). For all cosolvents, the main difference (some tenths of electrons) between GAFF2 or RESP and Mulliken is for carbon atoms and for hydrogen atoms directly bonded to them. Taking into account the main polarization effects, the Mulliken atomic charges are higher than those obtained through RESP method, determining more polar molecules. In fact, the resulting dipole moment was 2.66, 1.12, and

**TABLE 1** Calculated GAFF2 (G2), Mulliken (M), and RESP (R) atomic charges for TFE, HFIP, and HFA.

Atom	TFE			HFIP			HFA		
	G2(e)	M(e)	R(e)	G2(e)	M(e)	R(e)	G2(e)	M(e)	R(e)
C1	0.074	-0.280	0.098	0.657	1.011	0.536	0.680	1.095	0.618
C2	0.632	0.919	0.538	-0.004	-0.407	0.016	0.062	-0.228	0.228
C3	-	-	-	0.657	1.011	0.536	0.680	1.095	0.618
O1	-0.566	-0.651	-0.599	-0.543	-0.570	-0.545	-0.513	-0.605	-0.613
O2	-	-	-	-	-	-	-0.513	-0.605	-0.613
H1	0.077	0.243	0.093	0.133	0.301	0.192	0.447	0.545	0.472
H2	0.077	0.243	0.093	0.432	0.526	0.422	0.447	0.545	0.472
H3	0.417	0.510	0.419	-	-	-	-	-	-
F	-0.237	-0.328	-0.214	-0.222	-0.312	-0.193	-0.215	-0.307	-0.197

Note: For atom labeling, see Figure 1.

**TABLE 2** Computed (using the three sets of atomic charges) and experimental values for density (g/cm<sup>3</sup>) and static dielectric constant for pure solutions of TFE and HFIP.

	GAFF2	Mulliken	RESP	Experimental value <sup>52,53</sup>
Density $\rho$ (g/cm <sup>3</sup> )				
TFE	1.313 ± 0.013	1.475 ± 0.019	1.358 ± 0.015	1.383
HFIP	1.585 ± 0.008	1.712 ± 0.014	1.579 ± 0.008	1.607
Static dielectric constant, $\epsilon$				
TFE	12.4 ± 0.4	14.9 ± 0.9	13.4 ± 0.7	26.67
HFIP	6.1 ± 0.2	7.2 ± 0.5	4.6 ± 0.1	16.7

3.22 D with Mulliken and 2.31, 1.02, and 2.83 D with RESP for TFE, HFIP, and HFA, respectively.

### 3.2 | TFE and HFIP pure solutions

Using the three sets of atomic charges, we first performed MD simulations for pure solutions of TFE and HFIP. We did not take into account HFA since the mono-hydrate is solid at room temperature. We tested the ability of the new atomic charges to reproduce macroscopic observables as dielectric constant and density of pure solutions. The results are reported in Table 2.

GAFF2 and RESP atomic charges underestimate the density, and Mulliken atomic charges overestimate it. In the first case, we obtained a percentage error of at most 5%; the best density values are obtained with RESP atomic charges (percentage error of at most 1.8%). The overestimation of Mulliken atomic charges has a percentage error of 6%–7% for both solvents. The static dielectric constant is underestimated by the three sets of atomic charges with percentage errors higher than 40%. In this case, the best values are obtained with Mulliken atomic charges; for TFE and HFIP, a percentage error of 44.1% and 56.9%, respectively. The difference between computed and experimental  $\epsilon$  values was found also in previous studies and was ascribed to insufficient sampling and/or to the absence of an explicit polarization term in the FF.<sup>16,26</sup> Furthermore to obtain comparable values of  $\epsilon$  using MD simulation is not easy, as was pointed out also in a paper of Coleman et al.<sup>54</sup> in

which the dielectric constant has been defined “the hardest nut to crack.”<sup>55</sup>

To describe the liquid structure, we calculated the intermolecular radial distribution functions and the running integration number. The running integration number of  $g_{xy}(r)$  gives the average number of atoms  $y$  contained in a sphere of radius  $r$  centered on atom  $x$ . In Figure 2 (and below), we reported the results relative to RESP atomic charges; for the other two sets, the  $g(r)$ s are reported in Figures S1 and S2.

For TFE, the  $g_{O-H3}(r)$  gives a first peak at 1.87 Å with a running integration number of 0.74. The marked peak suggests the presence of an intermolecular hydrogen-bond network. A second coordination shell peak is at 3.55 Å with a running integration number of 2.08. The  $g_{F-H3}(r)$  does not have a well-defined peak; there is only a broad one at around 5.0 Å that could be due to the presence of different molecules in the network of O...H3 hydrogen bond. The  $g_{O-O}(r)$  shows a peak at 2.85 Å that is due to the hydrogen bond between O...H3. The same consideration can be done for  $g_{F-O}(r)$ . The  $g_{C1-C2}(r)$  (see Figure S4) presents an oscillating behavior and peaks at long distances due to long-range structural order. The  $g(r)$  is in agreement with Fioroni et al.'s data,<sup>16</sup> suggesting the presence of small clusters in which there are interactions between different -OH groups.

For HFIP, the  $g_{O-H2}(r)$  gives a first peak at 1.98 Å with a running integration number of 0.44 denoting the presence of a hydrogen bond interaction in which the reference molecule acts as hydrogen bond acceptor. The second peak at 3.55 Å with integration number 1.46 is due to a secondary interaction: There is the hydrogen bond

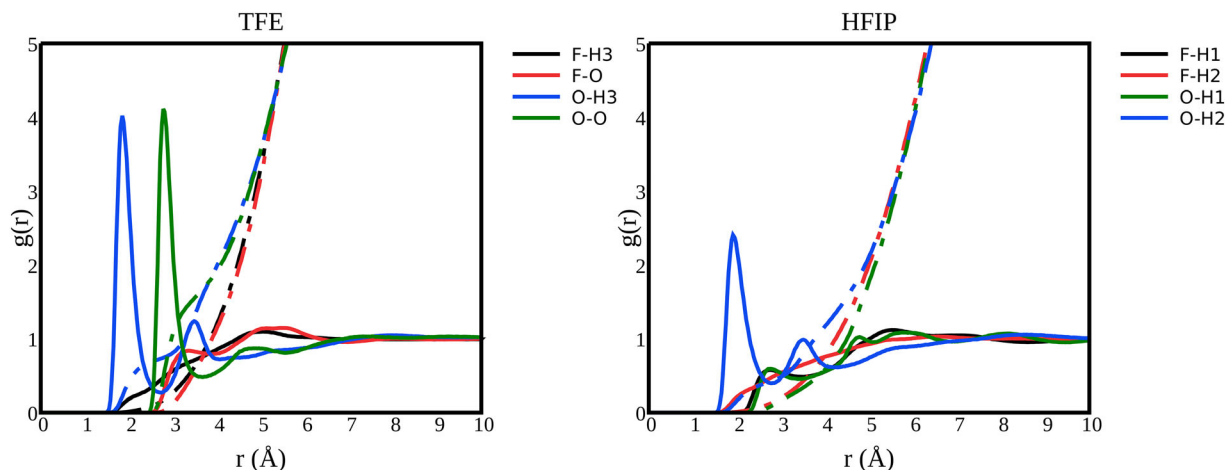


**FIGURE 2** Intermolecular radial distribution functions (continuous lines) and running integration number (dashed lines) between selected atoms of TFE (left) and HFIP (right) pure solutions calculated from MD simulations performed using RESP atomic charges.

	GAFF2	Mulliken	RESP	Experimental values <sup>4,52,53,56,57</sup>
$\Delta G_{\text{hydr}}(\text{kJ/mol})^{\text{a}}$				
TFE	$-13.55 \pm 0.27$	$-35.09 \pm 4.90$	$-15.41 \pm 0.31$	-18.0
HFIP	$-16.67 \pm 0.63$	$-35.21 \pm 0.62$	$-15.41 \pm 0.67$	-15.8
HFA	$-26.51 \pm 0.72$	$-24.15 \pm 2.60$	$-22.02 \pm 4.07$	-
Density, $\rho$ ( $\text{g/cm}^3$ ) <sup>b</sup>				
TFE	$1.136 \pm 0.14$	$1.206 \pm 0.13$	$1.159 \pm 0.13$	1.17
HFIP	$1.255 \pm 0.14$	$1.287 \pm 0.16$	$1.259 \pm 0.14$	1.25
HFA	$1.323 \pm 0.14$	$1.352 \pm 0.15$	$1.328 \pm 0.17$	-
Static dielectric constant, $\epsilon^{\text{b}}$				
TFE	$47.5 \pm 0.4$	$44.3 \pm 0.3$	$49.3 \pm 0.4$	48.15
HFIP	$41.5 \pm 0.5$	$41.5 \pm 0.2$	$38.9 \pm 0.4$	51.0
HFA	$34.5 \pm 0.6$	$37.4 \pm 0.4$	$33.2 \pm 0.3$	-

<sup>a</sup>The data are derived from the simulation of 1 cosolvent molecule and 500 water molecules.

<sup>b</sup>The data are derived from the simulation of 50:50 (v/v) water-cosolvent solution.

**TABLE 3** Computed (using the three sets of atomic charges) and experimental values for  $\Delta G_{\text{hydr}}$  (kJ/mol),  $\rho$  ( $\text{g/cm}^3$ ), and static dielectric constant for TFE, HFIP, and HFA.

defined by the first peak and the interaction between the oxygen atom and the hydrogen atom bonded to the interacting O. The other RDFs,  $g_{\text{F-H2}}(r)$ ,  $g_{\text{F-H1}}(r)$  and  $g_{\text{O-H1}}(r)$ , show only broad and small peaks.

Comparing Figure 2 and Figures S1 and S2, Mulliken atomic charges give stronger intermolecular interactions: The  $g(r)$ s peaks are higher and tighter in agreement with higher atomic charges and with the overestimation of density.

### 3.3 | TFE-, HFIP-, and HFA-water mixtures

One molecule of cosolvent was studied in a water solution; from the simulations, we estimated the  $\Delta G_{\text{hydr}}$  using FEP method, and the results are reported in Table 3. The experimental values are well reproduced when GAFF2 or RESP atomic charges are used. Very big

percentage errors occur with Mulliken atomic charges (percentage error of at least 90%). In Table 3, there are also the results relative to HFIP although the experimental counterpart is not available.

The other water solution considered is a water/cosolvent mixture 50:50 (v/v). We first computed macroscopic properties such as  $\rho$  and  $\epsilon$  and obtained the results shown in Table 3. For all sets of atomic charges, we obtained values in better agreement with experiments compared to the values obtained for pure solutions. For the density, the highest percentage error found is 3.1% (Mulliken atomic charges and TFE). For the static dielectric constant, the discrepancies are still high for Mulliken atomic charges, but for TFE, we find a very good agreement, with a percentage error of 2% and 1.8% for GAFF2 and RESP, respectively. For HFIP we found a higher percentage error but smaller respect to the one obtained for the estimation of pure solution. The GAFF2 and RESP atomic charges seem to better reproduce

the macroscopic properties. To achieve information on the accuracy of the cosolvent force field, an MD simulation on TFE/water mixture has been carried out by using SPC model for water. The dielectric constant computed for the new mixture is 40.0. This values can not be attributed only to the different dielectric constant of the two water models (94 and 65 for TIP3P and SPC, respectively<sup>58,59</sup>) but also to the intermolecular interactions, as it can be observed in Figure S5. However, since TIP3P is the most adopted water model in protein simulation, we decided to adopt this model in this study.

To verify the presence of a hydrogen bonding network between cosolvents and water molecules, we have analyzed the intermolecular  $g(r)$ , and in Figure 3, we have reported the data relative to RESP atomic charges. The other results are reported in Figures S6 and S7. For the TFE/water 50:50 (v/v) mixture, the  $g_{H3-Ow}(r)$  and  $g_{O1-Hw}(r)$  give a first peak at 1.9 Å and 2.02 Å, respectively, with a running integration number of 0.80 and 0.83. For intermolecular TFE interactions,  $g_{O1-H3}(r)$  gives a peak at 1.87 Å and an integration number of 0.13. Comparing the intensity of the different first peaks, we can conclude that there is a hydrogen bond network in which the TFE molecules act as hydrogen bond donors and the TFE molecules are surrounded by water molecules.

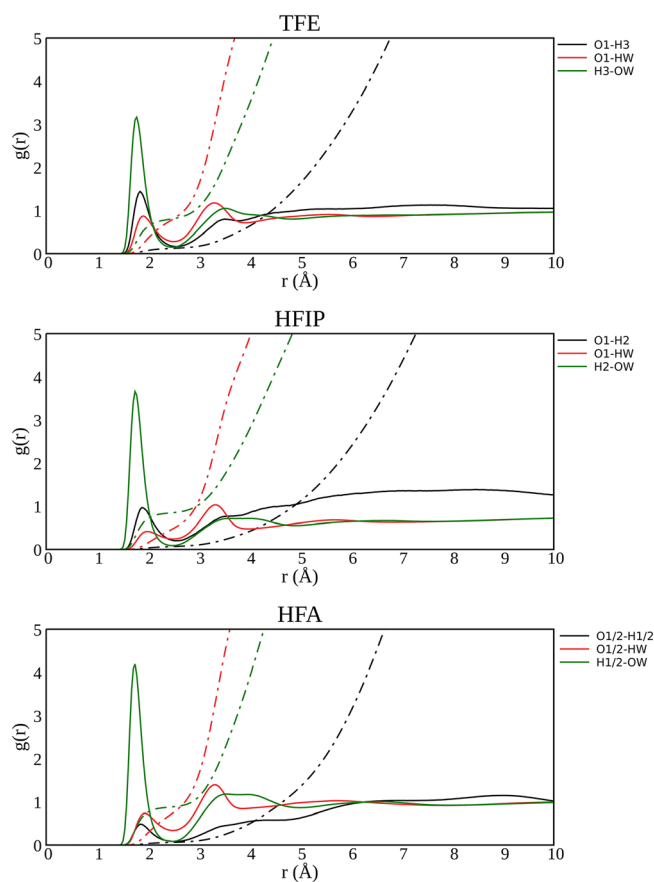


**FIGURE 3** Intermolecular pair distribution functions between selected atoms calculated from MD simulations performed using RESP atomic charges for the cosolvent/water 50:50 (v/v) mixtures. Top–bottom: TFE, HFIP, and HFA.

For HFIP/water 50:50 (v/v) mixture,  $g_{H2-Ow}(r)$  shows a sharp peak at 1.84 Å with a running integration number of 0.86. The other two  $g(r)$ s,  $g_{O1-Hw}$  and  $g_{O1-H2}$ , show smaller peaks at 2.02 Å and 1.96 Å, indicating that also in the case of HFIP/water mixture, the main interaction was between cosolvent and water molecules with HFIP as a donor of the hydrogen bond. The behavior of  $g_{O1-H2}$  can be explained by cluster formation.<sup>60,61</sup>

For HFA, as mentioned above, no references for macroscopic properties and MD simulations were found in the literature. The distributions of H1-O1-C2-C2 dihedral angles (see Figure S3) in the simulation of the HFA–water 50:50 (v/v) mixture do not show significant differences with those obtained from ab initio calculations (Figure 1). Our simulation suggests that the gem-diol interacts strongly with water. The structure of the mixture was studied by analyzing  $g(r)$  calculated between HFA hydrogen atoms and HFA and water oxygen atoms: The  $g_{H1/2-Ow}(r)$  shows a sharp peak at 1.77 Å with a running integration number of 0.88, while the  $g_{O1/2-Hw}(r)$  has a small first peak at 1.9 Å with a running integration number of 0.85 and a second peak is at 3.36 Å, which can be due to the  $g_{H1/2-Ow}(r)$ . The intermolecular HFA–HFA  $g_{O1/2-H1/2}(r)$  has a first small peak at 1.96 Å with a running integration number of 0.07 confirming that HFA also interacts mainly with water molecules.

Analyzing the structural information obtained with the other two sets of atomic charges (Figures S6 and S7), also for the cosolvent/water 50:50 (v/v) solutions, we obtain higher and tighter RDFs with Mulliken ones. Therefore, considering the current results, macroscopic properties and structural information are better described by RESP and GAFF2 atomic charges.

### 3.4 | Water–cosolvent mixtures/MLT simulations

The cosolvents are important because they affect the structure and dynamics of proteins and peptides. To verify the structure-inducing property, we simulated MLT in the cosolvent/water 50:50 (v/v) mixtures, and we compared the results with the simulation of aqueous solution. From the experiments,<sup>62</sup> it was found that the cosolvent molecules aggregate around the peptide chains. Furthermore, the structure of MLT in 35% HFIP/water solution is  $\alpha$ -helical between residues Ile-2 and Val-8 and from Leu-13 to Gln-26 with the connecting region from Leu-9 to Pro-14 in various turn conformations and probably quite flexible. A similar structure was found for MLT in 50% HFA/water solution with two  $\alpha$ -helical segments, one between residues Ala-4 and Thr-11 and one from Leu-13 to Arg-24, with a flexible connecting region.<sup>63,64</sup> To verify the structural stability of MLT, from the 100 ns of our simulations, we calculated the RMSD and the RMSF of the backbone (results in Figure 4) with respect to the NPT-equilibrated structure in both pure water and cosolvents/water mixtures. The RMSD shows similar behavior for TFE, HFIP, and HFA with a value within 5 Å for all simulations. The RMSD calculated for the MLT backbone in an aqueous solution shows higher values (about 11 Å after 37 ns of simulation) due to the unfolded structure. The flexibility of each residue was also evaluated using RMSF. The average

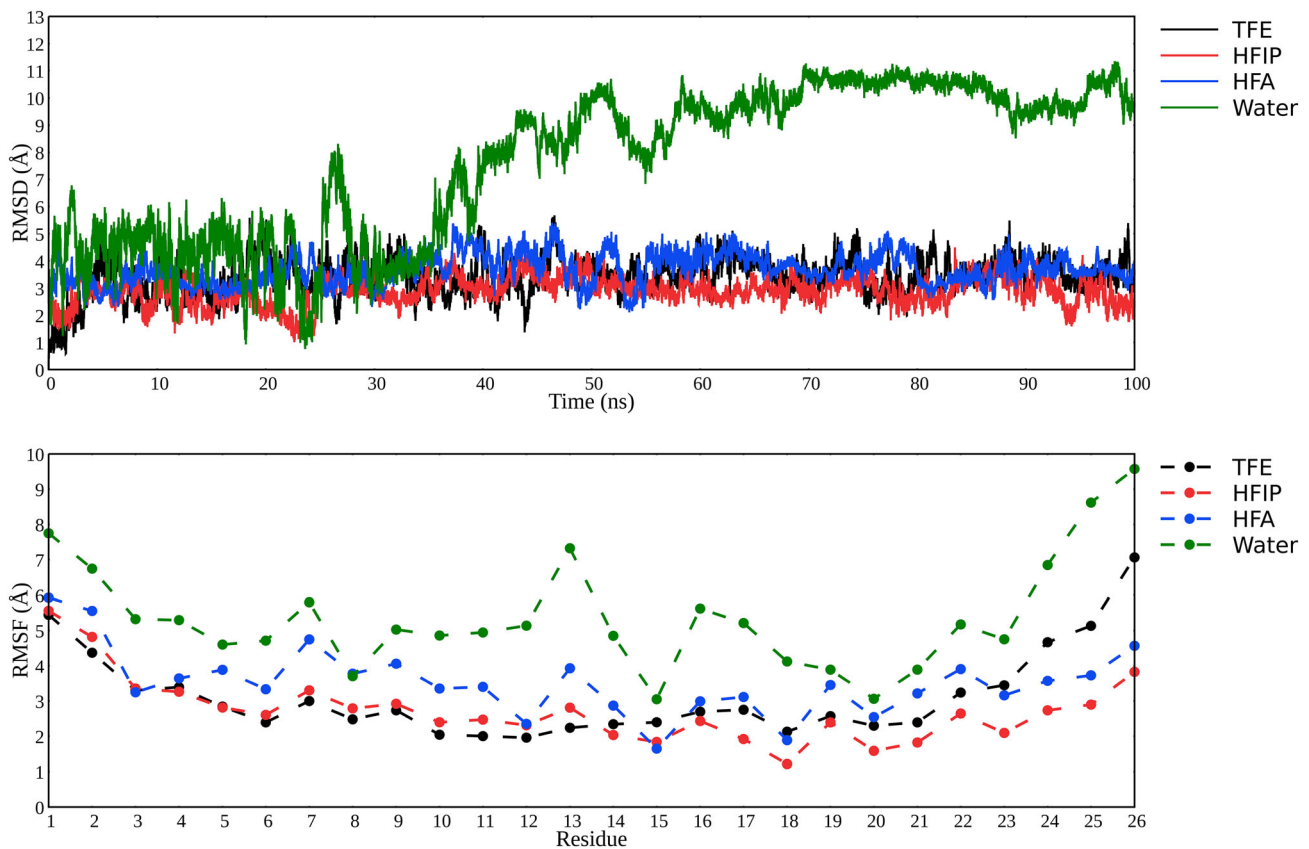


**FIGURE 4** RMSD (top) and RMSF (bottom) for MLT backbone in cosolvent/water 50:50 (v/v) solutions of TFE (black), HFIP (red), and HFA (blue) calculated from 100 ns of simulations. In green are results relative to MLT in aqueous solution.

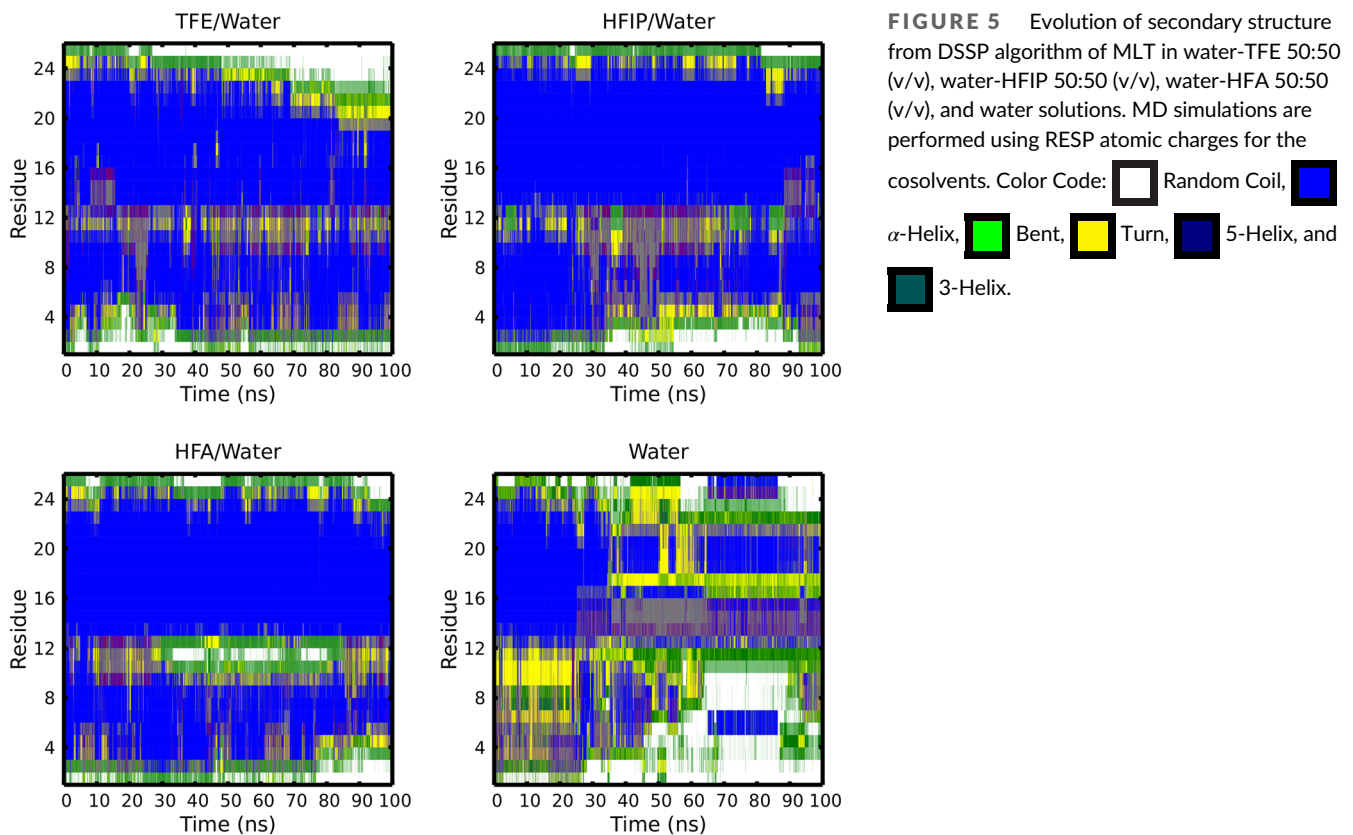
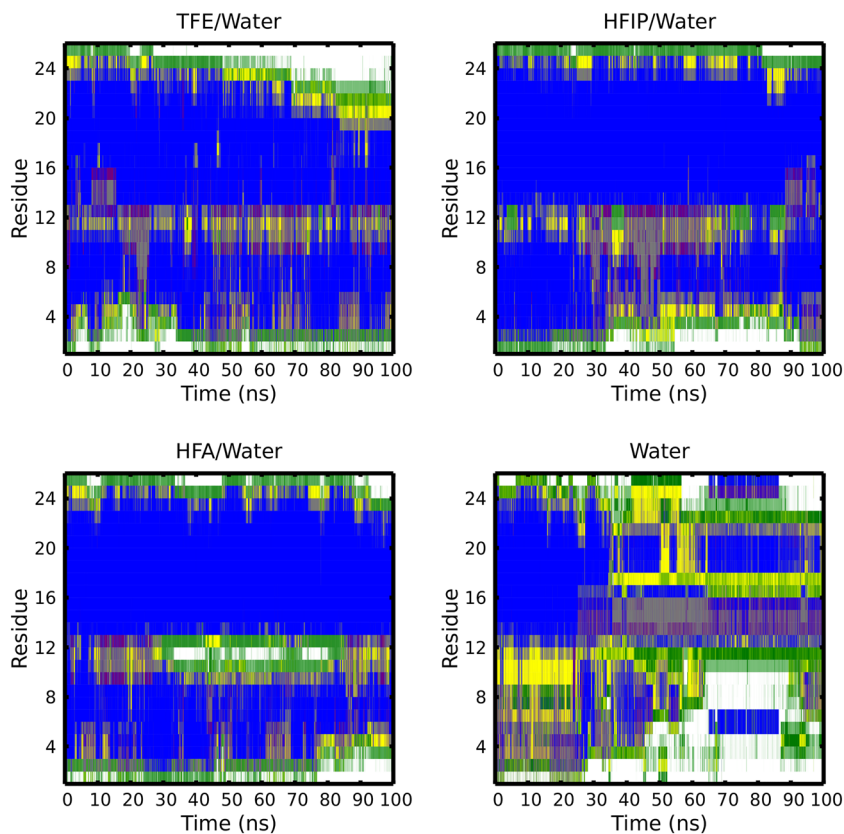


**FIGURE 5** Evolution of secondary structure from DSSP algorithm of MLT in water-TFE 50:50 (v/v), water-HFIP 50:50 (v/v), water-HFA 50:50 (v/v), and water solutions. MD simulations are performed using RESP atomic charges for the cosolvents. Color Code: Random Coil,  $\alpha$ -Helix, Bent, Turn, 5-Helix, and 3-Helix.



**FIGURE 6** Local cosolvent concentration for  $C_{\alpha}$  atom of each residue of MLT in cosolvent/water 50:50 (v/v) solutions of TFE (black), HFIP (red), and HFA (blu) at 6 Å. MD simulations are performed using RESP atomic charges for the cosolvents.



mobility of each residue in water is greater than that in the cosolvents/water mixture. Greater flexibility is marked for the central residue Leu-13, which is involved in the connection between the two  $\alpha$ -helical segments.

The secondary structure of MLT was studied with the DSSP algorithm (results for RESP atomic charges are in Figure 5).

For TFE and HFIP, a well-defined flexible region from Thr-11 to Leu-13 merges two stable  $\alpha$  helical regions. For HFA, the results are in agreement with the experimental data; two well-folded regions are enclosed between Ala-4 to Thr-11 and Leu-13 to Lys-23 with higher flexibility in the second helix end as reported also in RMSF. In addition, the DSSP calculated for MLT in aqueous solutions confirms the unstable structure already found in the RMSD analysis.

The MLT secondary structure obtained using GAFF2 atomic charges is more disordered, especially in HFIP/water 50:50 (v/v) solution and for the initial residues (from number 6) in the first 60 ns of the simulation (Figure S8). Also using Mulliken atomic charges, the MLT secondary structure is less stable in HFIP/water 50:50 (v/v) solution, and the  $\alpha$ -helix is loosened for residues from 1 to 7 and from 20 to 26 (Figure S9).

We calculated the LCC around the  $C_{\alpha}$  atom of each residue of MLT at 6 Å (Figure 6). For HFIP and TFE, the LCC at 6 Å has a trend consistent with the Roccatano et al.'s finding.<sup>9,10</sup> The LCC is similar to the bulk for the C-terminal portion, with a net decrease around the flexible region Thr-11 and Ile-20. The results for HFA are comparable with those of HFIP, with the tendency to aggregate decreases around Leu-9 and Thr-10 residues. The LCC for HFIP and HFA are also similar

when Mulliken and GAFF2 atomic charges (Figures S10 and S11) are used for these two cosolvents. A very different tendency was obtained when Mulliken atomic charges are used to simulate the TFE cosolvent.

In Figure S12, we have also reported the LCC calculated considering shells of variable size, from 4 Å to 25 Å. The MLT residues involved in the interactions with cosolvent molecules are the same for all cosolvents. HFIP aggregates at larger distances around MLT, high distances are also found for TFE, and HFA molecules are at smaller distances, around 12 Å. All these results confirm the structure-inducing property of the studied cosolvents especially when RESP atomic charges are used. In fact, the use of RESP atomic charges allows us to correctly describe the pure cosolvent, a cosolvent/water 50:50 (v/v) solution, and the structure-inducing property of the solvent.

## 4 | CONCLUSION

In this study, we have shown the results obtained by upgrading of the GAFF2 force field, with a reparameterization of the atomic charges of TFE, HFIP, and HFA fluorinated alcohols by ab initio calculations. Three different sets of atomic charges were tested (standard GAFF2, Mulliken, and RESP) and validated with MD simulations. The GAFF2 and RESP atomic charges give comparable results, which are in better agreement with experiments than the Mulliken atomic charges. In particular, the force field based on the standard GAFF2 parameters and

with RESP atomic charges reparameterization allows us to reproduce structural and macroscopic properties of pure and cosolvent/water 50:50 (v/v) mixtures. However, analyzing the solvent structure-inducing property, we conclude that RESP atomic charges provide slightly better results for all three solvents studied: TFE, HFIP, and HFA. The availability of several experimental data for TFE and HFIP allows us to compare MD results with experiments and to verify the accuracy of our computational approach. Furthermore, we can extend the same computational approach to generate a force field for HFA, for which no experimental or computational information are available.

## ACKNOWLEDGEMENTS

Authors acknowledge “Progetto Dipartimenti di Eccellenza 2018-2022” allocated to the Department of Chemistry “Ugo Schiff.” M.M., G.C., and M.P. thank the National Recovery and Resilience Plan, Mission 4 Component 2 - Investment 1.4 - NATIONAL CENTER FOR HPC, BIG DATA AND QUANTUM COMPUTING - funded by the European Union - NextGenerationEU - CUP B83C22002830001.

## ORCID

Michele Casoria  <https://orcid.org/0009-0007-2960-3971>

Marina Macchiagodena  <https://orcid.org/0000-0002-3151-718X>

Paolo Rovero  <https://orcid.org/0000-0001-9577-5228>

Claudia Andreini  <https://orcid.org/0000-0003-4329-8225>

Anna Maria Papini  <https://orcid.org/0000-0002-2947-7107>

Gianni Cardini  <https://orcid.org/0000-0002-7292-3555>

Marco Pagliari  <https://orcid.org/0000-0003-0240-161X>

## REFERENCES

- Buck M. Trifluoroethanol and colleagues: cosolvents come of age. recent studies with peptides and proteins. *Q Rev Biophys.* 1998;31(3): 297-355. doi:10.1017/S003358359800345X
- Searle MS, Zerella R, Williams DH, Packman LC. Native-like  $\beta$ -hairpin structure in an isolated fragment from ferredoxin: NMR and CD studies of solvent effects on the N-terminal 20 residues. *Protein Eng Des Sel.* 1996;9(7):559-565. doi:10.1093/protein/9.7.559
- Brown JE, Klee WA. Helix-coil transition of the isolated amino terminus of ribonuclease. *Biochemistry.* 1971;10(3):470-476. doi:10.1021/bi00779a019
- Hong D-P, Hoshino M, Kuboi R, Goto Y. Clustering of fluorine-substituted alcohols as a factor responsible for their marked effects on proteins and peptides. *J Am Chem Soc.* 1999;121(37):8427-8433. doi:10.1021/ja990833t
- Goodman M, Listowsky I. Conformational aspects of synthetic poly-peptides. VI. Hypochromic spectral studies of oligo- $\gamma$ -methyl-L-glutamate peptides. *J Am Chem Soc.* 1962;84(19):3770-3771. doi:10.1021/ja00878a036
- Barrow CJ, Yasuda A, Kenny PTM, Zagorski MG. Solution conformations and aggregational properties of synthetic amyloid  $\beta$ -peptides of Alzheimer's disease: analysis of circular dichroism spectra. *J Mol Biol.* 1992;225(4):1075-1093. doi:10.1016/0022-2836(92)90106-t
- Rajan R, Awasthi SK, Bhattacharjya S, Balaram P. “Teflon-coated peptides”: hexafluoroacetone trihydrate as a structure stabilizer for peptides. *Biopolymers.* 1997;42(2):125-128. doi:10.1002/(SICI)1097-0282(199708)42:2%3C125::AID-BIP1%3E3.0.CO;2-P
- Starzyk A, Barber-Armstrong W, Sridharan M, Decatur SM. Spectroscopic evidence for backbone desolvation of helical peptides by 2,2,2-trifluoroethanol: an isotope-edited FTIR study. *Biochemistry.* 2005;44(1):369-376. doi:10.1021/bi0481444
- Roccatano D, Colombo G, Fioroni M, Mark AE. Mechanism by which 2,2,2-trifluoroethanol/water mixtures stabilize secondary-structure formation in peptides: a molecular dynamics study. *Proc Natl Acad Sci USA.* 2002;99(19):12179-12184. doi:10.1073/pnas.182199699
- Roccatano D, Fioroni M, Zacharias M, Colombo G. Effect of hexa-fluoroisopropanol alcohol on the structure of melittin: a molecular dynamics simulation study. *Protein Sci.* 2005;14(10):2582-2589. doi:10.1110/ps.051426605
- Van Buuren AR, Berendsen HJC. Molecular dynamics simulation of the stability of a 22-residue  $\alpha$ -helix in water and 30% trifluoroethanol. *Biopolymers.* 1993;33(8):1159-1166. doi:10.1002/bip.360330802
- Van Gunsteren WF, Berendsen HJC. Groningen molecular simulation (GROMOS) library manual, bioms b.v.: Groningen.
- Radnai T, Ishiguro S, Ohtaki H. Intramolecular and liquid structure of 2,2,2-trifluoroethanol by X-ray diffraction. *J Solut Chem.* 1989;18(8): 771-784. doi:10.1007/BF00651809
- Bodkin MJ, Goodfellow JM. Hydrophobic solvation in aqueous tri-fluoroethanol solution. *Biopolymers.* 1996;39(1):43-50. doi:10.1002/(SICI)1097-0282(199607)39:1%3C43::AID-BIP5%3E3.0.CO;2-V
- Van Gunsteren WF, Billeter SR, Eising AA, et al. Biomolecular simulation: The GROMOS96 manual and user guide; vdf Hochschulverlag AG an der ETH Zürich and Bioms b.v.: Zürich, Groningen; 1996.
- Fioroni M, Burger K, Mark AE, Roccatano D. A new 2,2,2-trifluoroethanol model for molecular dynamics simulations. *J Phys Chem B.* 2000;104(51):12347-12354. doi:10.1021/jp002115v
- Chitra R, Smith PE. A comparison of the properties of 2,2,2-trifluoroethanol and 2,2,2-trifluoroethanol/water mixtures using different force fields. *J Chem Phys.* 2001;115(12):5521-5530. doi:10.1063/1.1396676
- Scharge T, Cézard C, Zielke P, Schütz A, Emmeluth C, Suhm MA. A peptide cosolvent under scrutiny: self-aggregation of 2,2,2-trifluoroethanol. *Phys Chem Chem Phys.* 2007;9(32):4472-4490. doi:10.1039/B705498J
- Ponder JW, Case DA. Force fields for protein simulations. *Protein simulations*, Advances in Protein Chemistry, vol. 66: Academic Press; 2003:27-85. <https://www.sciencedirect.com/science/article/pii/S006532330366002X>
- Tian C, Kasavajhala K, Belfon KAA, et al. ff19SB: amino-acid-specific protein backbone parameters trained against quantum mechanics energy surfaces in solution. *J Chem Theory Comput.* 2020;16(1):528-552. doi:10.1021/acs.jctc.9b00591
- Jia X, Zhang JZH, Mei Y. Assessing the accuracy of the general AMBER force field for 2,2,2-trifluoroethanol as solvent. *J Mol Model.* 2013;19(6):2355-2361. doi:10.1007/s00894-013-1776-1
- Wang J, Wolf RM, Caldwell JW, Kollman PA, Case DA. Development and testing of a general AMBER force field. *J Comput Chem.* 2004; 25(9):1157-1174. doi:10.1002/jcc.20035
- Vymetal J, Vondrásek J. Parametrization of 2,2,2-trifluoroethanol based on the generalized AMBER force field provides realistic agreement between experimental and calculated properties of pure liquid as well as water-mixed solutions. *J Phys Chem B.* 2014;118(35):10390-10404. doi:10.1021/jp505861b
- Vega C, Abascal JLF, Nezbeda I. Vapor-liquid equilibria from the triple point up to the critical point for the new generation of TIP4P-like models: TIP4P/Ew, TIP4P/2005, and TIP4P/ice. *J Chem Phys.* 2006; 125(3):34503. doi:10.1063/1.2215612
- Kinugawa K, Nakanishi K. Molecular dynamics simulations on the hydration of fluoroalcohols. *J Chem Phys.* 1988;89(9):5834-5842. doi:10.1063/1.455534
- Fioroni M, Burger K, Mark AE, Roccatano D. Model of 1,1,1,3,3,3-hexafluoro-propan-2-ol for molecular dynamics simulations. *J Phys Chem B.* 2001;105(44):10967-10975. doi:10.1021/jp012476q

27. Murto J, Kivinen A, Lundström G. Part 14.1 Densities, refractive indices, viscosities, and isothermal vapour-liquid equilibria of hexafluoroacetone-water mixtures. *Acta Chem Scand.* 1971;25(7):6. doi:10.3891/acta.chem.scand.25-2451
28. Tayyari SF, Gholamhoseinpour M, Emamian S, Sammelson RE. Conformational analysis, structure, and normal coordinate analysis of vibrational spectra of hexafluoroacetone. A density functional theory study. *J Fluor Chem.* 2016;184:65-71. doi:10.1016/j.jfluchem.2016.02.013
29. Lindorff-Larsen K, Piana S, Palmo K, et al. Improved side-chain torsion potentials for the AMBER ff99SB protein force field. *Proteins.* 2010;78(8):1950-1958. doi:10.1002/prot.22711
30. Kemple MD, Buckley P, Yuan P, Prendergast FG. Main chain and side chain dynamics of peptides in liquid solution from <sup>13</sup>C NMR: melittin as a model peptide. *Biochemistry.* 1997;36(7):1678-1688. doi:10.1021/bi962146%2B
31. Hirota N, Mizuno K, Goto Y. Group additive contributions to the alcohol-induced  $\alpha$ -helix formation of melittin: implication for the mechanism of the alcohol effects on proteins. *J Mol Biol.* 1998;275(2):365-378. doi:10.1006/jmbi.1997.1468
32. Marsili S, Signorini GF, Chelli R, Marchi M, Procacci P. ORAC: a molecular dynamics simulation program to explore free energy surfaces in biomolecular systems at the atomistic level. *J Comput Chem.* 2010;31(5):1106-1116. doi:10.1002/jcc.21388
33. Procacci P. PrimaDORAC: a free web interface for the assignment of partial charges, chemical topology, and bonded parameters in organic or drug molecules. *J Chem Inf Model.* 2017;57(6):1240-1245. doi:10.1021/acs.jcim.7b00145
34. Bayly CI, Cieplak P, Cornell W, Kollman PA. A well-behaved electrostatic potential based method using charge restraints for deriving atomic charges: the resp model. *J Phys Chem.* 1993;97(40):10269-10280. doi:10.1021/j100142a004
35. Pagliai M, Funghi G, Vasseti D, Procacci P, Chelli R, Cardini G. Imidazole in aqueous solution: hydrogen bond interactions and structural reorganization with concentration. *J Phys Chem B.* 2019;123(18):4055-4064. doi:10.1021/acs.jpcc.9b01611
36. Frisch MJ, Trucks GW, Schlegel HB, et al. Gaussian 09. Gaussian Inc. Wallingford CT 2016.
37. Barone V, Cossi M. Quantum calculation of molecular energies and energy gradients in solution by a conductor solvent model. *J Phys Chem A.* 1998;102(11):1995-2001. doi:10.1021/jp9716997
38. Wang J, Cieplak P, Kollman PA. How well does a restrained electrostatic potential (resp) model perform in calculating conformational energies of organic and biological molecules? *J Comput Chem.* 2000;21(12):1049-1074.
39. Abraham MJ, Murtola T, Schulz R, et al. Gromacs: High performance molecular simulations through multi-level parallelism from laptops to supercomputers. *SoftwareX.* 2015;1-2:19-25. doi:10.1016/j.softx.2015.06.001
40. Jorgensen WL, Chandrasekhar J, Madura JD, Impey RW, Klein ML. Comparison of simple potential functions for simulating liquid water. *J Chem Phys.* 1983;79(2):926-935. doi:10.1063/1.445869
41. Pagliai M, Macchiagodena M, Procacci P, Cardini G. Evidence of a low-high density turning point in liquid water at ordinary temperature under pressure: a molecular dynamics study. *J Phys Chem Lett.* 2019;10(20):6414-6418. doi:10.1021/acs.jpcclett.9b02724
42. Nosé S. A molecular dynamics method for simulations in the canonical ensemble. *Mol Phys.* 1984;52(2):255-268. doi:10.1080/00268970110089108
43. Parrinello M, Rahman A. Strain fluctuations and elastic constants. *J Chem Phys.* 1982;76(5):2662-2666. doi:10.1063/1.443248
44. Darden T, York D, Pedersen L. Particle mesh Ewald: An N-log(N) method for Ewald sums in large systems. *J Chem Phys.* 1993;98(12):10089-10092. doi:10.1063/1.464397
45. Allen MP, Tildesley DJ. *Computer Simulation of Liquids*: Press, OC; 1987.
46. Hess B, Bekker H, Berendsen HJC, Fraaije JGEM. Lincs: a linear constraint solver for molecular simulations. *J Comput Chem.* 1997;18(12):1463-1472. doi:10.1002/(SICI)1096-987X(199709)18:12%3C1463::AID-JCC4%3E3.0.CO;2-H
47. Beutler TC, Mark AE, van Schaik RC, Gerber PR, van Gunsteren WF. Avoiding singularities and numerical instabilities in free energy calculations based on molecular simulations. *Chem Phys Lett.* 1994;222(6):529-539. doi:10.1016/0009-2614(94)00397-1
48. Bennett CH. Efficient estimation of free energy differences from monte carlo data. *J Comput Phys.* 1976;22:245-268. doi:10.1016/0021-9991(76)90078-4
49. Brehm M, Thomas M, Gehrke S, Kirchner B. TRAVIS—a free analyzer for trajectories from molecular simulation. *J Chem Phys.* 2020;152(16):164105. doi:10.1063/5.0005078
50. Hollóczki O, Macchiagodena M, Weber H, et al. Triphasic ionic-liquid mixtures: fluorinated and non-fluorinated aprotic ionic-liquid mixtures. *Chem Phys Chem.* 2015;16(15):3325-3333. doi:10.1002/cphc.201500473
51. Kabsch W, Sander C. Dictionary of protein secondary structure: Pattern recognition of hydrogen-bonded and geometrical features. *Biopolymers.* 1983;22(12):2577-2637. doi:10.1002/bip.360221211
52. Madelung O. Static dielectric constants of pure liquids and binary liquid mixtures. *Numer Data Funct Relation Sci Technol.* 1991;6:459. doi:10.1007/b44266
53. Rochester CH, Symonds JR. Densities of solutions of four fluoroalcohols in water. *J Fluorine Chem.* 1974;4(2):141-148. doi:10.1016/S0022-1139(00)82508-7
54. Caleman C, van Maaren PJ, Hong M, Hub JS, Costa LT, van der Spoel D. Force field benchmark of organic liquids: density, enthalpy of vaporization, heat capacities, surface tension, isothermal compressibility, volumetric expansion coefficient, and dielectric constant. *J Chem Theory Comput.* 2012;8(1):61-74. doi:10.1021/ct200731v
55. Macchiagodena M, Mancini G, Pagliai M, Barone V. Accurate prediction of bulk properties in hydrogen bonded liquids: amides as case studies. *Phys Chem Chem Phys.* 2016;18:25342-25354. doi:10.1039/C6CP04666E
56. Cabani S, Gianni P, Mollica V, Lepori L. Group contributions to the thermodynamic properties of non-ionic organic solutes in dilute aqueous solution. *J Solut Chem.* 1981;10:563-595. doi:10.1007/BF00646936
57. Marenich AV, Kelly CP, Thompson JD, et al. Minnesota Solvation Database (MNSOL) version 2012. doi:10.13020/3eks-j059; 2020.
58. Izadi S, Onufriev AV. Accuracy limit of rigid 3-point water models. *J Chem Phys.* 2016;145(7):74501. doi:10.1063/1.4960175
59. van der Spoel D, Van Maaren PJ, Berendsen HJC. A systematic study of water models for molecular simulation: derivation of water models optimized for use with a reaction field. *J Chem Phys.* 1998;108(24):10220-10230. doi:10.1063/1.476482
60. Kuprin S, Graslund A, Ehrenberg A, Koch MHJ. Nonideality of water-hexafluoropropanol mixtures as studied by X-ray small angle scattering. *Biochem Biophys Res Commun.* 1995;217(3):1151-1156. doi:10.1006/bbrc.1995.2889
61. Ramos-Villaseñor JM, Rodríguez-Cárdenas E, Dáaz1 CEB, Frontana-Urbe BA. Review—use of 1,1,1,3,3,3-hexafluoro-2-propanol (HFIP) co-solvent mixtures in organic electrosynthesis. *J Electrochem Soc.* 2020;167:155509. doi:10.1149/1945-7111/abb83c
62. Neuman Jr RC, Gerig JT. Interactions of 2,2,2-trifluoroethanol with melittin. *Magn Reson Chem.* 2009;47(11):925-931. doi:10.1002/mrc.2489

63. Gerig JT. Structure and solvation of melittin in 1,1,1,3,3,3-hexafluoro-2-propanol/water. *Biophys J*. 2004;86(5):3166-3175. doi:[10.1016/S0006-3495\(04\)74364-7](https://doi.org/10.1016/S0006-3495(04)74364-7)
64. Gerig JT. Structure and solvation of melittin in hexafluoroacetone/water. *Biopolymers*. 2004;74(3):240-247. doi:[10.1002/bip.20085](https://doi.org/10.1002/bip.20085)

#### SUPPORTING INFORMATION

Additional supporting information can be found online in the Supporting Information section at the end of this article.

**How to cite this article:** Casoria M, Macchiagodena M, Rovero P, et al. Upgrading of the general AMBER force field 2 for fluorinated alcohol biosolvents: A validation for water solutions and melittin solvation. *J Pept Sci*. 2023;e3543. doi:[10.1002/psc.3543](https://doi.org/10.1002/psc.3543)